Vol 16 No 4, April 2007
1009-1963/2007/16(04)/1155-04

Chinese Physics

© 2007 Chin. Phys. Soc.
and IOP Publishing Ltd

Laser-diode excited intense upconversion luminescence of Er^{3+} in bismuth–lead–germanate glasses*

Li Tao(李 涛)[a)†], Zhang Qin-Yuan(张勤远)[b)†], and Jiang Zhong-Hong(姜中宏)[b)]

[a)] *College of Science, South China Agriculture University, Guangzhou* 510640, *China*

[b)] *Key Laboratory of Specially Functional Materials and Advanced Manufacturing Technology, Ministry of Education, Institute of Optical Communication Materials, South China University of Technology, Guangzhou* 510640, *China*

(Received 15 August 2006; revised manuscript received 10 November 2006)

We have investigated infrared-to-visible upconversion luminescence of Er^{3+} in bismuth–lead–germanate glasses. The UV cutoff wavelength is shortened while its lifetime is increased almost linearly, with PbF_2 substituting for PbO in the bismuth–lead–germanate glasses. Three emissions centred at around 529, 545 and 657 nm are clearly observed, which are identified as originating from the $^2H_{11/2} \rightarrow {}^4I_{15/2}$, $^4S_{3/2} \rightarrow {}^4I_{15/2}$ and $^4F_{9/2} \rightarrow {}^4I_{15/2}$ transitions, respectively. It is noted that all the upconversion emission intensities increase with PbF_2 concentration increasing. The ratio between the intensities of red and green emissions increases with the increasing of PbF_2 content. Energy transfer processes and nonradiative phonon-assisted decays account for the populations of the $^2H_{11/2}$, $^4S_{3/2}$ and $^4F_{9/2}$ levels. The quadratic dependence of fluorescence on excitation laser power confirms a two-photon process to contribute to the upconversion emissions.

Keywords: upconversion, luminescence, Er^{3+}, bismuth–lead–germanate glasses

PACC: 7820, 4270C, 7840

1. Introduction

The availability of commercial high-power infrared (IR) laser diodes (LD) in recent years has prompted researches on the visible upconversion lasers which have potential applications in numerous photonic devices including three-dimensional laser displays, high-density data storage, high-resolution printing, medical diagnostics and undersea communications. The glasses are particularly attractive hosts because they are easy to be made into various shapes, such as optical fibres and planar waveguides, and doped by different rare-earth (RE) ions with various concentrations, compared with crystals.[1] Specially, RE-doped optical glass fibre can confine the pumping energy from the laser diodes efficiently and maintain a high intensity over a long interaction length; besides, it can be better applied to medical diagnostics and optical communication.[2,3] Er^{3+} ions are the most studied among the RE ions because Er^{3+}-doped materials exhibit a strong luminescence in the visible and infrared regions, and these transitions can be enhanced by using appropriate host materials.[4–9] The matrix for Er^{3+} plays an important role in achieving the high-efficient upconversion emission because the optical properties of RE ions are effectively influenced by the ligand field and the vibration property of the host; especially, the maximum phonon energy of the glass network can largely affect the upconversion efficiency by multiphonon relaxation.[10,11] An Er^{3+}-doped fluoride glass systems have been exhibited to effectively emit an IR-to-visible upconversion fluorescence compared with most of oxide glass systems, since their lower phonon energy reduce the nonradiative loss caused by the multiphonon relaxation process.[4,12] However, their relatively low chemical durability and thermal stability and the difficulty in their fabrication have so far hindered fluoride glasses from being applied commercially.[13] Oxyfluoride glass has been identified as a candidate for upconversion fluorescence materials, which is designed for improving the thermal stability and chemical durability of fluoride-based glasses.[14] Among the oxide glasses, lead germanate glasses are of growing interest because they combine high mechanical strength and high chemical durability and thermal stability with

*Project supported by the National Natural Science Foundation of China (Grant No 50472053), the Programme for New-Century Excellent Talents in Universities of Ministry of Education, China (Grant No NCET-04-0823) and the Natural Science Foundation of Guangdong Province, China (Grant No 04020036).

†Corresponding author. E-mail: pzhlee@126.com, qyzhang@scut.edu.cn

excellent transmission in the IR region up to 4.5 μm and low phonon energy $\sim 800\,\mathrm{cm}^{-1}$.[15–17] In this paper, we report on the infrared-to-visible upconversion luminescence observed in Er^{3+} in the GeO_2–Bi_2O_3–PbO–PbF_2 (GBPP) glasses and the effect of PbF_2 on upconversion luminescence of Er^{3+} in the GBPP glasses.

2. Experimental procedure

GBPP glasses with the molar composition of $62GeO_2 \cdot 25Bi_2O_3 \cdot (13-x)PbO \cdot xPbF_2$ ($x = 0, 4, 8,$ and 13 mol.%) were prepared using reagent-grade powders. The Er^{3+} doping concentration in the glasses was 2 mol.%, which was introduced as Er_2O_3 with 99.99% purity. Samples are named as described in Table 1 in order to recognize the composition easily. The required quantity of raw materials was well mixed in an agate mortar and melted in a platinum crucible at 1000–1100 °C for 20 min, and then quenched on preheated stainless steel blocks. After being annealed, samples were polished and cut into pieces, each having a size of $10 \times 10 \times 2\,\mathrm{mm}^3$.

Table 1. Densities, refractive indices and Er^{3+} concentrations of Er^{3+}-doped $62GeO_2 \cdot 25Bi_2O_3 \cdot (13-x)PbO \cdot xPbF_2$ ($x = 0$, 4, 8, and 13 mol.%) glasses.

Sample	x/mol.%	Density/(g/cm^3)	Refractive index	Er^{3+} concentration/$10^{20}\,\mathrm{cm}^{-3}$
GBPP0	0	6.923	1.896	3.93
GBPP4	4	6.963	1.890	3.94
GBPP8	8	6.978	1.889	3.93
GBPP13	13	6.925	1.885	3.88

The densities of the glasses were measured by using Archimedes' method. The Er^{3+} concentrations were calculated from the initial molar compositions and the measured sample densities. The refractive indices were determined on prism by using the minimum deviation method. The glass densities, refractive indices, and Er^{3+} concentrations of the samples are summarized in Table 1.

Absorption spectra were determined by a Perkin-Elmer Lambda-900 UV/VIS/NIR spectrophotometer ranging from 380 to 1700 nm with a resolution of 1 nm. Fluorescence spectra were measured on a TRIAX320 spectrofluorimeter with a 977 nm laser diode as an excitation source. Fluorescence lifetimes were measured using a modulated source and a computer controlled digitizing oscilloscope. All the measurements were performed at room temperature.

3. Results and discussion

For the absorption measurements, we obtain the spectra of the Er^{3+}-doped $62GeO_2 \cdot 25Bi_2O_3 \cdot (13-x)PbO \cdot xPbF_2$ (mol.%) shown in Fig.1. Each assignment corresponds to the excited level of Er^{3+}. The substitution of PbF_2 affects the transmittances in $62GeO_2 \cdot 25Bi_2O_3 \cdot (13-x)PbO \cdot xPbF_2$ (mol.%) as demonstrated in Fig.2. The peaks of all the curves refer to the Er^{3+} absorption band. It is obvious that the UV cutoff wavelength is shortened, with PbF_2 substituting for PbO, as can be seen in Figs.1 and 2. Extrapolating to zero transmittance at the steepest slope, the cutoff wavelengths for $x = 0, 4, 8,$ and 13 are estimated to be 404, 401, 399, and 395 nm, respectively.

Figure 3 shows the measured lifetimes of the Er^{3+}: $^4I_{13/2}$ level in the glasses with different PbF_2 contents at room temperature. It is clearly seen that the lifetime increases almost linearly with the increase of PbF_2 concentration. The lifetime for $x = 13$ exhibits a maximum value of 5.16 ms. This behaviour may result from the decrease of the hydroxyl groups which is due to the reaction of fluoride groups, with PbF_2 substituting for PbO.[18] Hydroxyl groups in glasses could effectively quench lifetime of Er^{3+}: $^4I_{13/2}$ level.[19]

The upconversion emission spectra of $62GeO_2 \cdot 25Bi_2O_3 \cdot (13-x)PbO \cdot xPbF_2$(mol.%) in a visible range of 500–750 nm under the 977 nm excitation are shown in Fig.4. Three emissions centred at around 529, 545 and 657 nm are clearly observed, which are identified as originating from the $^2H_{11/2} \rightarrow {}^4I_{15/2}$, $^4S_{3/2} \rightarrow {}^4I_{15/2}$ and $^4F_{9/2} \rightarrow {}^4I_{15/2}$ transitions of Er^{3+}, respectively. All the transitions increase as the PbF_2 concentration increases, which might be due to the influence of PbF_2 on the maximum phonon energies of the glasses.[20] The PbO-free GBPP13 glass shows a very intense upconversion luminescence, especially. The ratio between the integrated intensities of red and green emis-

sions (R/G) increases swiftly from 0.58 of $x = 0$ to 1.32 of $x = 13$ in the presence of PbF_2. The figure and data suggest that the substitution of PbF_2 for PbO_2 has a less effect on the green emissions than the red emission.

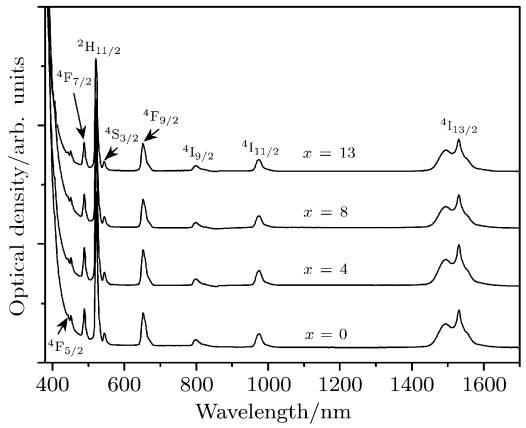


Fig.1. Absorption spectra of Er^{3+}-doped $62GeO_2 \cdot 25Bi_2O_3 \cdot (13 - x)PbO \cdot xPbF_2$ ($x = 0$, 4, 8, and 13 mol.%) glasses. The assignments of absorption bands are indicated by the excited level.

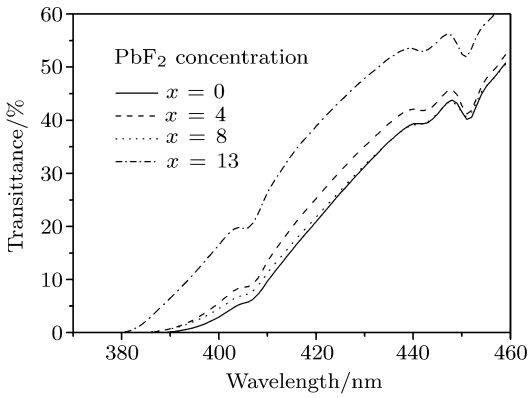


Fig.2. Wavelength-dependent transmittances in the Er^{3+}-doped $62GeO_2 \cdot 25Bi_2O_3 \cdot (13 - x)PbO \cdot xPbF_2$ ($x = 0$, 4, 8, and 13 mol.%) glasses.

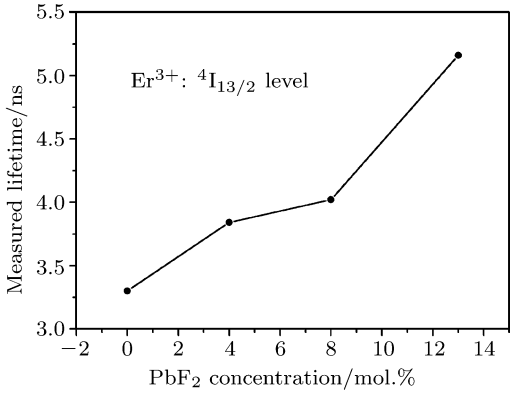


Fig.3. Effect of the substitution of PbF_2 on lifetime of the Er^{3+}: $^4I_{13/2}$ level in Er^{3+}-doped $62GeO_2 \cdot 25Bi_2O_3 \cdot (13-x)PbO \cdot xPbF_2$ (mol.%) glasses.

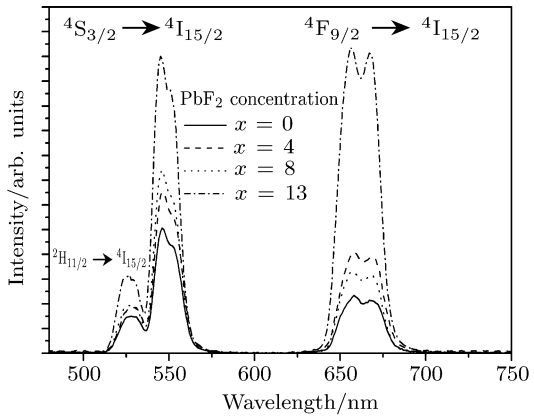


Fig.4. IR-to-visible upconversion luminescence spectra of the Er^{3+}-doped $62GeO_2 \cdot 25Bi_2O_3 \cdot (13 - x)PbO \cdot xPbF_2$ (mol.%) glasses upon the 977 nm excitation.

In the frequency upconversion process, the upconversion emission intensity I_{UP} is proportional to I_{IR}^n, where I_{IR} and n represent the IR excitation intensity and the number of IR photons absorbed per visible photon emitted, respectively.[21,22] Figure 5 shows the logarithmic dependence of upconversion emission intensity of the GBPP13 glass on pump laser power upon the 977 nm excitation. A plot of log I_{UP} versus log I_{IR} yields a straight line with a slope n. The obtained values of n are 2.14, 2.10 and 2.03 for 529, 545 and 657 nm emissions, respectively. These slopes confirm that two photons significantly contribute to the visible upconversion luminescence. The possible upconversion mechanisms of three upconversion processes are shown in the inset of Fig.5. Energy transfer processes and nonradiative phonon-assisted decays account for the populations of the $^2H_{11/2}$, $^4S_{3/2}$ and $^4F_{9/2}$ levels.[17] The transitions from the $^2H_{11/2}$, $^4S_{3/2}$ and $^4F_{9/2}$ states to the $^4I_{15/2}$ state show the 529, 545 and 657 nm emissions, respectively.

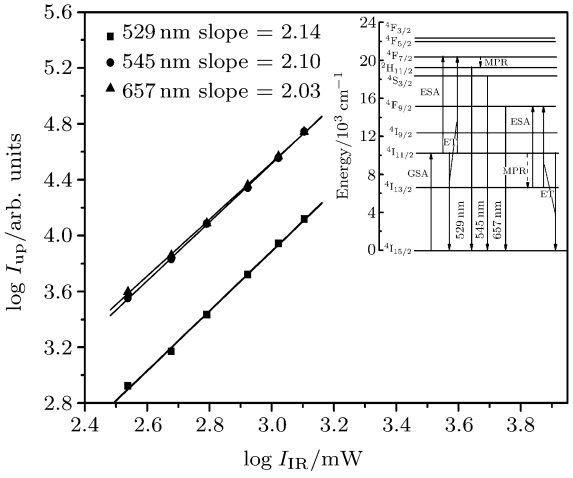


Fig.5. Dependence of the upconversion emission intensity on excitation power in Er^{3+}-doped GBPP13 glass. The inset shows energy level diagram of possible upconversion mechanisms.

4. Conclusions

In summary, IR-to-visible frequency upconversions in Er^{3+}-doped bismuth–lead–germanate heavy metal oxide glasses have been investigated experimentally. The UV cutoff wavelength is shortened while its lifetime is increased almost linearly, with PbF_2 substituting for PbO in the bismuth–lead–germanate glasses. Intense upconversion emissions centred at around 529, 545 and 657 nm, corresponding to the $^2H_{11/2} \rightarrow {}^4I_{15/2}$, $^4S_{3/2} \rightarrow {}^4I_{15/2}$ and $^4F_{9/2} \rightarrow {}^4I_{15/2}$ transitions of Er^{3+} respectively, are observed upon the excitation of 977 nm LD. All the upconverted transitions increase with PbF_2 concentration increasing. The substitution of PbF_2 for PbO has a less effect on the green emissions. The results show that the Er^{3+}-doped bismuth–lead–germanate heavy metal oxide glasses could be a promising candidate for applications in upconversion based optical devices.

References

[1] Miyajima Y, Komukai T and Sugawa T 1994 *Opt. Fiber Technol.* **1** 35

[2] Tanabe S, Yoshii S, Hirao K and Soga N 1992 *Phys. Rev.* B **45** 4620

[3] Joubert M F 1999 *Opt. Mater.* **11** 181

[4] Oliveira A S, de Araujo M T, Gouveia-Neto A S, Medeiros Neto J A, Sombra A S B and Messaddeq Y 1998 *Appl. Phys. Lett.* **72** 753

[5] Li T, Zhang Q Y and Jiang Z H 2006 *Acta Phys. Sin.* **55** 4298 (in Chinese)

[6] Liu Y H, Chen D D, Hou Z Y, Chen H, Zhang Q Y, Deng Z D and Jiang Z H 2005 *Acta Phys. Sin.* **54** 422 (in Chinese)

[7] Vetrone F, Boyer J C, Capobianco J A, Speghini A and Bettinelli M 2002 *Appl. Phys. Lett.* **80** 1752

[8] Zou X and Izumitani T 1993 *J. Non-Cryst. Solids* **162** 68

[9] Shojiya M, Takahashi M, Kanno R, Kawamoto Y and Kadono K 1995 *Appl. Phys. Lett.* **67** 2453

[10] Liu Y H, Chen D D, Zhang Q Y and Jiang Z H 2006 *Opt. Mater.* **28** 302

[11] Araújo C B de, Meneses L S, Maciel G S, Acioli L H, Gomes A S L, Messaddeq Y and Aegerter M A 2002 *Appl. Phys. Lett.* **68** 602

[12] Ronchin S, Rolli R, Montagna M, Duverger C, Tikhomirov V, Jha A, Ferrari M, Righini G C, Pelli S and Fossi M 2001 *J. Non-Cryst. Solids* **284** 243

[13] Pan Z, Morgan S H, Loper A, King V, Long B H and Collins W E 1995 *J. Appl. Phys.* **77** 4688

[14] Wen L, Yang J H and Hu L L 2004 *Acta Phys. Sin.* **53** 4378 (in Chinese)

[15] Wachtler M, Speghini A, Gatterer K, Fritzer H P, AjòD and Bettinelli M 1998 *J. Am. Ceram. Soc.* **81** 2045

[16] Balda R, Fernández J, Arriandiage M A and Fdez-Navarro J M 2004 *Opt. Mater.* **25** 157

[17] Sun H T, Zhang L Y, Liao M S, Zhou G, Yu C L, Zhang J J, Hu L L and Jiang Z H 2006 *J. Lumin.* **117** 179

[18] Ebendorff-Heidepriem H, Seeber W and Ehrt D 1993 *J. Non-Cryst. Solids* **163** 74

[19] Jiang Y S, Daniel R and Wu R K 1995 *Chin. J. Laser* B **4** 307

[20] Zhang Q Y, Li T, Shi D M, Yang G F, Yang Z M, Jiang Z H and Buddhudu S 2006 *J. Appl. Phys.* **99** 033510

[21] Muller P, Wermuth M and Gudel H U 1998 *Chem. Phys. Lett.* **190** 105

[22] Pollnau M and Gamelin D R 2000 *Phys. Rev.* B **61** 3337